Thermal-hydraulic two-phase modeling of Reactivity-Initiated transients with CATHARE2 -application to SPERT-IV simulation

J-M Labit, N Seiler, O Clamens, E Merle

Thermal-hydraulic two-phase modeling of Reactivity-Initiated transients with CATHARE2 - application to SPERT-IV simulation

J-M. Labit, N. Seiler[1], O. Clamens[1] and E. Merle[2]
[1]CEA, DES, IRESNE
Cadarache F-13108 Saint Paul-Lez-Durance, France

[2]CNRS-IN2P3-LPSC/Grenoble INP/UGA
53 Rue des Martyrs, 38026 Grenoble Cedex, France

jean-marc.labit@cea.fr

May 17, 2021

Abstract

Reactivity-Initiated Accidents (RIA) in nuclear reactor cores are very complex multiphysic transients. They consist in a very fast power excursion in the core, leading to wall temperature excursions. Many experiments have shown that the heat exchanges coefficients during fast transients differ from those in steady-states. The thermal-hydraulic phenomenology of such transients remains complex and some experimental studies allowed to better understand and quantify the heat exchanges between the wall and the fluid, for both single and two-phase flows.

The current study lies in a continuous effort of developing and validating a coupled neutronic and thermal-hydraulic code for the analysis of protected and unprotected transient behavior of reactors. More specifically, this study deals with the extension of the thermal hydraulic model of the CATHARE2 code to fast transient configurations. The extended CATHARE2 model is validated against experimental results from SPERT-IV. This reactor was driven mainly by the coolant density reactivity feedback. Thanks to that, many flow regimes can be observed in the core during the transient. That allows a more accurate evaluation of the adequacy of available transient two-phase flow models and correlations. The results, that represent the state of modeling, allow concluding that introduced models in CATHARE2 are able to simulate RIA tests such as SPERT-IV involving fast transient boiling.

Keywords— SPERT-IV, transient heat exchanges, boiling regime, Reactivity-Initiated Transients, CATHARE

Nomenclature

Acronyms

BE	Best Estimate
BEPU	Best Estimate Plus Uncertainty
BWR	Boiling Water Reactor
CABRI	French experimental reactor dedicated to safety studies

CATHARE	Code for Analysis of THermalhydraulics during an Accident of Reactor and safety Evaluation
CEA	Commissariat à l'Energie Atomique et aux Energies Alternatives (French Alternative Energies and Atomic Energy Commission)
CHF	Critical Heat Flux
DNB	Departure from Nucleate Boiling
EDF	Electricité De France
FDNB	Fully Developed Nucleate Boiling
IAEA	International Atomic Energy Agency
IRSN	Institut de Radioprotection et de Sûreté nucléaire (Institute for Radiological protection and Nuclear Safety)
MIT	Massachusetts Institute of Technology
NSRR	Nuclear Safety Research Reactor
ONB	Onset of Nucleate Boiling
OV	Overshoot
PWR	Pressurized Water Reactor
QPIRT	Quantified Phenomena Identification Ranking Table
RBMK	Reaktor Bolschoi Moschtschnosti Kanalny
RI	Reactivity Insertion
RIA	Reactivity-Initiated Accident
SFR	Sodium Fast Reactor
SPC	Single Phase Convection
SPERT	Special Power Excursion Reactor Test
VVER	Water Water Energy Reactor

Mathematical operators and variables

Δ	Difference

Physical variables

α	Thermal diffusion coefficient of water ($m^2.s^{-1}$)
λ	Conductivity ($W.m^{-1}.K^{-1}$)
ϕ	Heat flux ($W.m^{-2}$)
ρ	Density ($kg.m^{-3}$)
σ	Standard deviation or Surface tension (N/m)
τ	Heat flux excursion period (s)
c_p	Heat capacity ($J.kg^{-1}.K^{-1}$)
D_h	Hydraulic diameter (m)
h	Heat exchange coefficient ($W.m^{-2}.K^{-1}$)
Nu	Nusselt number
P	Volumetric power
Pr	Prandtl number
r	Cavity radius (m)
Re	Reynolds number
t	Time (s)

T, P, G	Temperature (K), pressure (Pa), mass flow rate (kg/s)
X_{th}	Thermodynamic quality
Subscripts	
0	First order or initial
1	Beginning of the wall heat flux excursion
2	End of the wall heat flux excursion
∞	In the bulk
c	Cavity of a nucleation site
$conv$	Convection
$crit$	Critical
l	Liquid
ONB	Onset of Nucleate Boiling
sat	Saturation
sub	Subcooling
w	Wall

1 Introduction

This modeling and validation work forms a part of a large effort leading to the improvement and the validation of the multi-physics modeling of Reactivity-Initiated Accidents with the system tool CATHARE2 [1].

This type of accident must be considered in the safety analysis of nuclear reactors and research reactors. Multi-physic benchmarks, proposed by IAEA (International Atomic Energy Agency), are based on experimental data deduced from experiments performed in research reactors. Series of such benchmarks were made available in the framework of the IAEA CRP 1496 [2] and were published in 2015 as IAEA Technical Reports Series No. 480 [3]. The report contains experimental data gathered from different research reactors such as ETRR-2 (Egypt), IEA-R1 (Brazil), Minerve (France), SPERT-III and IV (USA), and more. The report includes Reactivity-Initiated Accident experimental measured data and is intended to be used as a code validation benchmark [4]. CATHARE2 (Code for Analysis of Thermal Hydraulics during Accident of Reactor and Safety Evaluation) [1] has been developed by four French partners: CEA, IRSN, EDF and FRAMATOME. This highly verified and validated tool is intended, among other things, for safety analyses with best estimate calculations of thermal-hydraulics transients in PWRs for postulated accidents or other incidents and quantification of conservative margins. The description of thermal non-equilibrium inhomogeneous two-phase flow is based on a two-fluid approach and a six-equation model, using mainly algebraic constitutive relations for the modeling of interfacial coupling, of wall friction, and of wall heat transfer processes. This tool is able to model any kind of experimental facility or PWR (western type or VVER), and is usable for other reactors (fusion reactor, RBMK, BWR, research reactor, SFR). Unfortunately, it is not adapted and thus validated for the simulation of very fast reactivity insertion transients yet (order of magnitude between one and hundred of milliseconds) [1]. The final challenge is thus to succeed the simulation of the various multi-physics reactivity insertion transients catching the governing multi-physic phenomena with this CATHARE2 tool. These RI transients embrace fast phenomena under thermal-hydraulics, thermal-mechanics and neutronics coupling. After having reviewed the current capabilities of the CATHARE2 tool in regard to the main influential phenomena occurring during such RI transients (established from a QPIRT), many improvements have been achieved [5–7]; notably the improvement of the neutronic point-kinetics method to handle 3D effects in the core (where even if the evolutions of the radial and axial profiles or neutron spectrum evolution during the transient are not simulated, all major feedback effects are computed in a 3D way with a differential method), the coupled modeling of the reactor core with the transient rods circuit, the thermo-mechanical model describing the evolution of the conductance of the gap between the pellet and the clad *etc.* The clad-to-coolant heat transfer during fast transient in liquid single phase has also been improved in [6]. This extended version of CATHARE2 has been validated on various RIA tests

realized in the CABRI reactor involving fast transients under single-phase liquid flow regimes [5]. However, most correlations for boiling regimes used in system or component thermal-hydraulics simulation tools are still issued from steady-state experiments. This is the case in CATHARE2 [1], RELAP5 [8], ATHLET [9] and TRACE [10]. However, plotting such models (the steady-state dotted curve in fig. 1) and RI-related experimental data on the same map shows a huge difference: the heat fluxes and temperature ranges of each regime differ significantly between the power transient case and the steady-state case described in the literature.

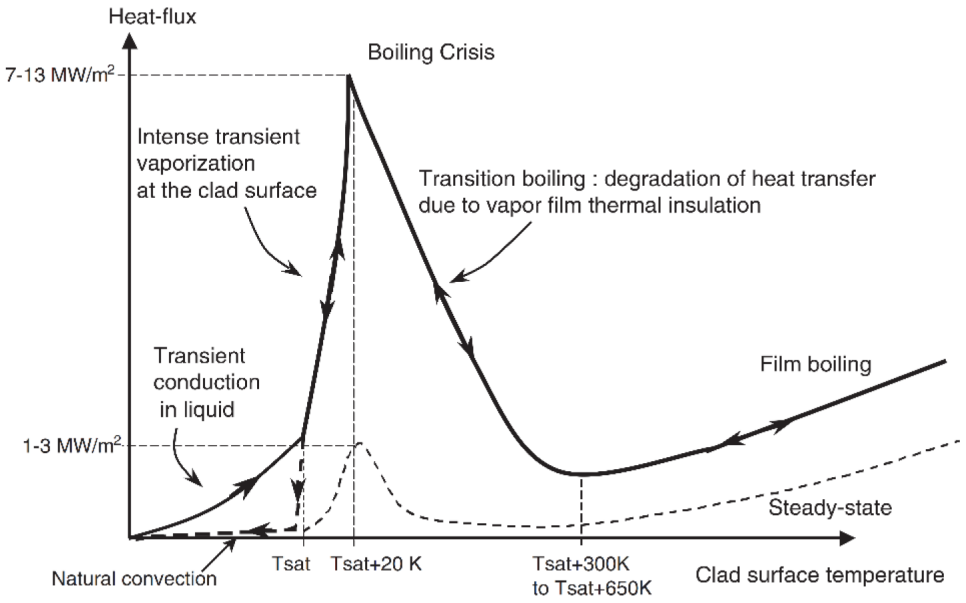

Figure 1: Schematic view of the experimental boiling curve in the fast RIA NSRR tests [11]

The next challenge for the simulation of complex fast RI transients in research reactors is the modeling and the validation of the heat transfers in transient boiling regimes which have a huge impact on the heat fluxes (fig. 1). Nevertheless, the CABRI reactor is not a adapted tool for the validation of these heat transfers. Indeed, in the CABRI reactor the low enriched fuel presents a large $^{238}U/^{235}U$ ratio which enables a sufficient Doppler-feedback effect to drop the power before coolant boiling. The fast power transients performed in the CABRI reactor do not lead to significant coolant boiling. That is why the CABRI experiments cannot be used to validate the fast transients heat transfers correlations. Whereas, in some other research reactors, like SPERT-IV for example, where the $^{238}U/^{235}U$ ratio is very small, the Doppler feedback effect is practically eliminated and the reactivity coefficient of the coolant/moderator is emphasized. Thus in case of reactivity insertion, the fuel temperature continues to increase exponentially while the coolant remains liquid. And, as the subcooling is high, the liquid water temperature does not increase enough for the moderator effect to stop the power excursion before boiling inception. After boiling inception, heat transfer at the wall increases significantly during nucleate boiling and void appears in the channels. This induces a stronger moderator feedback. The power excursion being mitigated, the heat flux drops down and so the void produced. Consequently, the neutronic moderation also decreases; that might allow a new power excursion as observed in SPERT-IV experiment [12].

This paper deals with the boiling regimes modeling under fast transient and their validation on SPERT-IV tests. The unique combination of highly enriched Uranium fuel and large reactivity insertion makes of SPERT-IV a good validation database for two-phase heat transfers in fast transients. The SPERT-IV experiment aimed at studying the dynamic behavior of a research reactor system by the performance and analysis of reactor kinetic experiments. The SPERT-IV D-12/25 core was the final aluminum plate-type core studied as part of the Special Power Excursion Reactor Test (SPERT) project. The experimental details are summarized in section 4.1. Thus the characteristics of these experiments provide a good (and still challenging) platform for the evaluation of extended two-phase flow models introduced in CATHARE2.

The difficulty of simulating transient heat exchanges in boiling regimes has been highlighted by Badrun and al. [13] who carried out EUREKA-2/RR [14] simulations for SPERT-IV reactor benchmark calculations against the experimental results provided by IAEA. The tests from B20 to B39, that fall under only forced convection mode, have been considered for simulation. Also, Woodruff at al. [15] compared results of RELAP5/MOD3 and PARET/ANL codes with the experimental transient data from the SPERT-IV D-12/25 series. And Chatzidakis and al. paid a special attention to the modeling of a SPERT-IV experiment under different departure from nucleate boiling correlations [4]. Finally Margulis and Gilad [16] validated an extension of the thermal-hydraulic model to the two-phase flow regime of the THERMO-T code on SPERT-IV D12/15 transients. They considered a coupling between a neutron point kinetics model and a homogeneous two-phase flow model with a commonly utilized correlations for the estimation of the onset of the significant void point, of the void fraction correlation and of the drift flux velocity model. Only SPERT-IV tests presenting low reactivity insertions were considered (less than 1.2 $) due to the limitations of the models, especially the rapid evaporation of the coolant which was not modeled. The results obtained showed a large deviation between the experimental and calculated results for all the cases. The differences concerned the entire transient period, with large temperature deviations, although the global trend of the calculated results is similar to the experimental one. Their results fell in line with results obtained from the previous evaluations made with PARET-ANL and RELAP5 [15], where large discrepancies were also observed. They concluded that their homogeneous approach for two-phase modeling is probably not sufficient for the simulation of the SPERT-IV experiments, and a more sophisticated model is required.

The final aim of this research work is to improve the reactors code modeling and to assess and qualify computational codes for application in the safety analysis of various research reactors under fast transients. This paper first describes the different models that have been developed for flow boiling regimes in fast transients and implemented in the extended CATHARE2 code. In order to assess the relevancy of these physical models, the SPERT-IV reactor has been modeled with CATHARE2. The SPERT-IV tests and the CATHARE2 code are presented in section 4.1. Five simulations of the SPERT-IV tests, presenting the highest reactivity insertion in each group of coolant flow conditions, are compared to experimental results and discussed; one of them fall under natural circulation (section 5). Finally, conclusions are drawn on the validation state of this extended CATHARE2 code for fast RI transients.

2 Experimental studies and existing physical models

In this section, an overview on the heat transfer regimes is presented as well as some existing experimental studies and models. Boiling heat transfers have been widely investigated as it is involved in many industrial processes from heat exchangers to quenching in metallurgy. The complexity due to the different involved mechanisms (local heat transfer, phase change, multi-phase flow) induces many challenges to understand the underlying physics and models even in steady state. The underlying physics understanding and the experiments achievement are ever harder in fast transient conditions. Some experimental studies have then been led in this field: early studies [17–19] and more recent ones [20–23]. The objective of these experiments was to quantify the heat exchanges in the different flow regimes during wall heat flux excursions. The experiments led in the MIT (Massachusetts Institute of Technology) [20–23] consisted of a wall heated with an exponential power source and exchanging energy with water, that can been stagnant as well as in forced convection. Its aim was to experimentally study both single and two phase heat exchanges between the heating wall and the water in fast transient conditions. The power source delivered a thermal power of exponential shapes like $e^{t/\tau}$ with different wall heat flux excursions period noted τ.

First in this section, these experiments are described as well as the main outcomes they brought in terms of understanding and models. In the next section 3, correlations are confronted to results of these past experimental studies and implemented in CATHARE2. They allow to model the boiling curve in transient condition up to the critical heat flux (fig. 1).

2.1 Single phase heat exchanges

Before approaching convection effect on heat exchanges, some studies have been made in order to study heat transfers in a pure conductive way.

From these conductive studies detailed in [20], it can be deduced that the transient can be separated into two main steps.

- First, when the wall temperature increases, the thermal boundary layer grows.
- Then, this thermal boundary layer reaches a maximum thickness whereas the heat flux keeps increasing.

Sakuraï [17] and Su et al. [21] both show that the wall temperature reaches an asymptotic behavior (*i.e.* when transient time tends to infinity, defined in [21] as $t > 3\tau$) proportional to the asymptotic heat flux. This implies that the heat exchange coefficient reaches a finite and non-zero asymptotic limit value depending on the excursion period τ.

Other studies have been led in order to study convection effect on heat exchanges during fast transients [21]. Experimental conditions are the same as in [20] but an adding cooling loop provides different Reynolds numbers and a manageable subcooling of the fluid in front of the wall. The objective is to study the effect of the subcooling and of the Reynolds number on the transient heat exchanges, that are driven by both pure transient conduction and convection. The authors concluded that the single phase pure convection is the overlap of two main mechanisms: the advection (wall axial supply in upstream cold water) and the turbulent mixing in the boundary layer. This latter phenomenon is due to vortexes in boundary layers inducing radial mixing through the velocity boundary layer. Su et al. [20] show that, in most cases involving turbulent flows, the turbulent mixing phenomenon is preponderant, because the vorticity time scale into the boundary layer is smaller than the advection time scale.
To these mechanisms, is added a pure conduction heat exchange mechanism through the thermal boundary layer. Convection and conduction overlap and are modeled as a conducto-convective heat transfer coefficient given in [21].

2.2 Onset of Nucleate Boiling

The Onset of Nucleate Boiling (ONB) corresponds to the transition from single-phase to fully developed nucleate boiling (FDNB) regime. This transition is also difficult to model in steady-state. Indeed, when a minimum wall superheat is reached, bubbles start to nucleate at the surface of the heated wall. Nucleation occurs preferentially at some specific locations of the surface called nucleation sites. The activation of the nucleation sites is a complex phenomenon depending on the wall superheat and surface conditions (roughness and wettability).
In transient conditions, among the results from [17, 20], two types of transitions at nucleate boiling onset have been observed:

- An evolution of heat flux with strong inertial effect, due to a low excursion period (and then a very fast high flux excursion) and a high subcooling. It leads to a local temperature maximum called overshoot (OV) at boiling inception. Indeed, when the heat flux increases after the onset of boiling driven regime, the wall temperature decreases before the beginning of the depletion of the liquid superheated layer at the wall, and increases again after this point (left part in fig. 2);
- An evolution of heat flux with low inertial effect, characterized by high excursion period and low subcooling. This curve is then similar to the boiling curve in steady state (right part in fig. 2).

Similarly, in the experiments [20,21] the onset of boiling driven regime is obtained for higher wall superheat if τ decreases or if the subcooling increases. The nominal values of this point of ONB and their trends with subcooling, with Reynolds number and with the heat flux excursion period are confirmed by a theoretical analysis similar to the one suggested by Sakuraï [17] based on the equilibrium of a bubble in a nucleation site [24] (see section 3). The main conclusions are that the wall super-heat at ONB decreases with the excursion period τ (for given Re and ΔT_{sub}) and can reach values of ~ 40°C for $\tau \approx 5$ ms, as illustrated in fig. 3.

2.3 Fully Developed Nucleate Boiling

Concerning the heat exchanges in the Fully Developed Nucleate Boiling regime, Su et al. [21] show that, at a given subcooling, the heat exchanges do not depend on the excursion period or of the Reynolds number. The

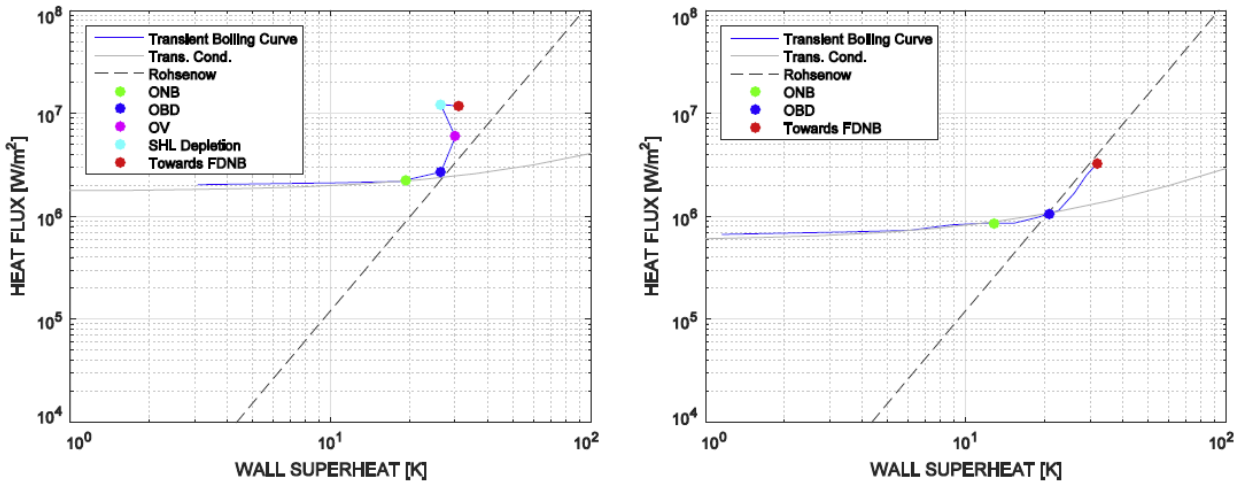

Figure 2: Two types of transition mechanisms from single-phase to FDNB
FDNB=Fully Developed Nucleate Boiling which could be approached in steady-state by the Rohsenow model, SHL: SuperHeated Layer [21]

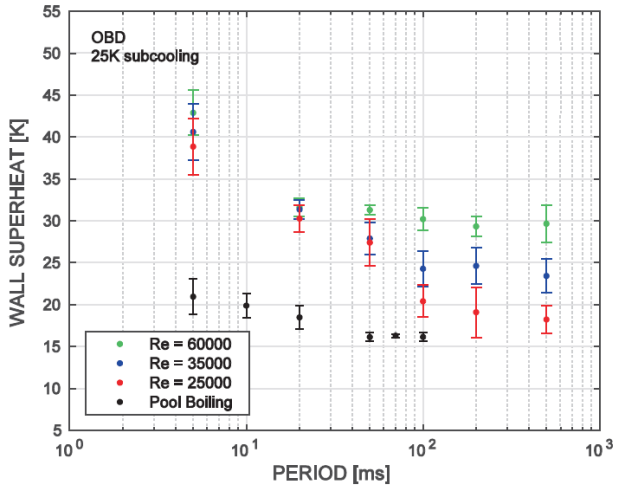

Figure 3: ONB point [21]

boiling curve trends towards the "steady-state" boiling curve. A correlation similar to Jens-Lottes correlation catches this behavior [25] (cf. fig. 4).

2.4 Departure from Nucleate Boiling (DNB) and Critical Heat Flux (CHF)

The objective of past tests was to quantify the critical heat flux during RIA. Some results come from NSRR tests (Nuclear Safety Research Reactor) [26] and from the experimental tests performed by Sakuraï [18, 27] and more recent ones [22]. The main observations were that:

- the critical heat flux decreases with the heat flux excursion period τ [18, 22];
- the critical heat flux increases with the subcooling [18, 22];
- for very low excursion periods, the transient critical heat flux does not depend on the Reynolds number any more [22];

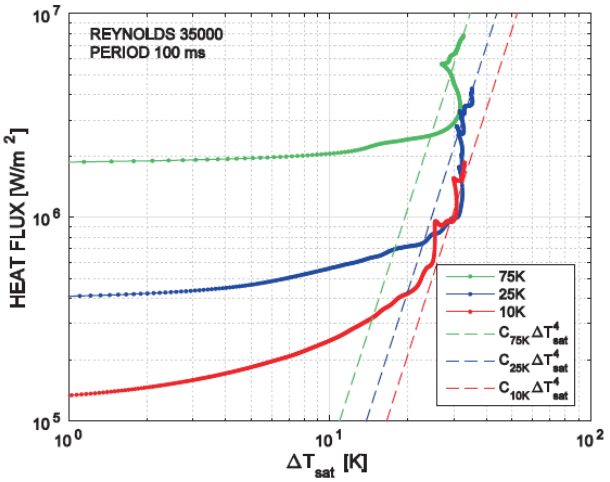

Figure 4: Fully Developed Nucleate Boiling regime. Dotted lines are Jens-Lottes correlation [21]

- the mechanism of DNB is similar as it is in steady-state: bubbles grow at the wall, fuse together until dry-out;
- more generally, the critical heat flux is greater in fast transient [23] than in steady-state.

More recently, experimental studies have been carried out by CEA and MIT on the transient critical heat flux [28]. They have reported that the impact of pressure cannot be investigated independently of the temperature, either considering constant bulk temperature or subcooling. The conditions of high subcooling and strong forced convection highly differentiate the behaviors and the dominant mechanisms from pool boiling, subcooling or saturation. The dependency on the power escalation period of the transient CHF highly depends on the flow conditions. At high subcooling, the boiling heat transfer is a wall phenomenon. Nucleation and Condensation Cycles efficiently transfer the heat from the wall to a neighbouring layer of liquid. The boiling crisis is triggered when this layer reaches the saturation temperature. The exploitation of their model has shown that the transient behavior of the system cannot be predicted only with the power escalation period. The heated length, the channel width and the flow conditions should be also considered.

3 Developed correlations for transient heat transfers

This section deals with the different correlations and models that have been developed on the basis of the experiments whose results are available in [20–22]. The objectives and main features of the modeling are summarized in fig. 5. The boiling curve (up to the DNB) in transient conditions is completely described by:

- a single phase heat exchange coefficient in single phase regime noted $h(t, \tau, \Delta T_{sub}, Re)$;
- the ONB occurrence, defined by $\Delta T_{sat_{ONB}}$;
- after this point, for simplification purpose, the overshoot (OV) is not modeled and the flow regime is considered to be in Fully-Developed Nucleate Boiling and characterized by the heat flux $\phi_{NB}(T_{ONB}, \Delta T_{sub}, T_w - T_{sat})$;
- the CHF occurrence at the DNB noted $\phi_{crit}(\tau, \Delta T_{sub}, P, G, X_{th})$;

The transition boiling regime occurring for wall temperatures higher than the DNB in transient heat flux excursion are not modeled yet and the steady-state models are kept in CATHARE2 for these regimes. In fig. 5 are outlined the experimental (black curve) and the modeled (red curve) wall heat flux evolution against the wall super-heat. .

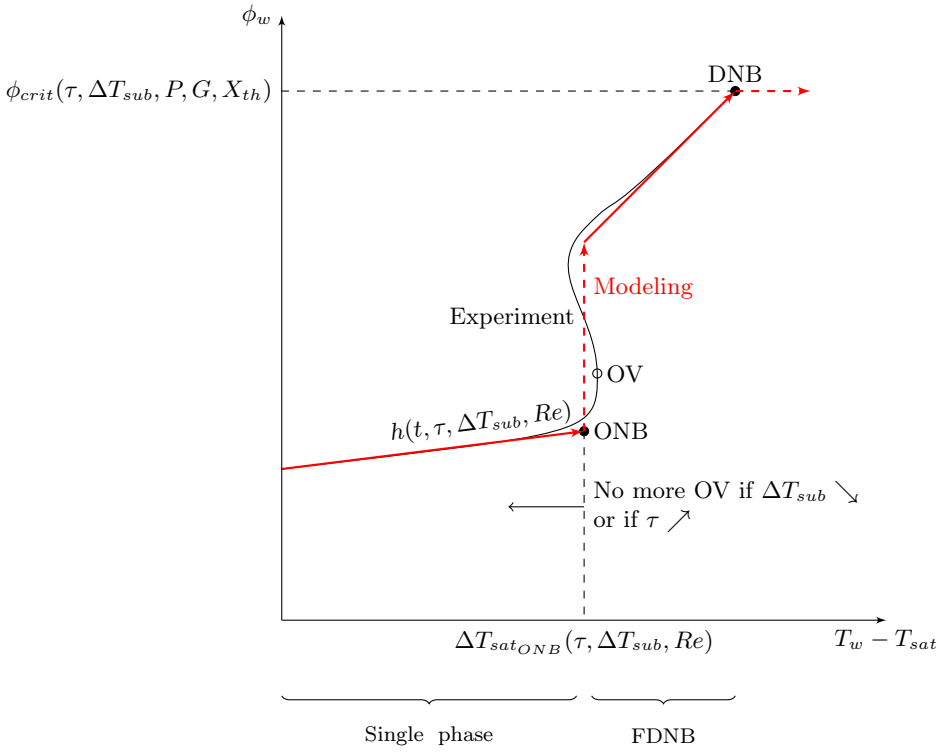

Figure 5: Principles of thermal-hydraulics modeling in CATHARE2 for RIA studies

3.1 Single phase transient heat exchanges

The single phase heat transfer modeling in transient conditions issue has already been addressed in [6] and the derived correlation (1) has been successfully implemented in CATHARE2. This single phase heat transfer results of the superposition of transient conductive and pure steady-state convective heat exchanges. Analytical calculations allowed to determine a conductive heat exchange during the different phases of the transient displayed in fig.6: an exponential excursion of the wall heat flux followed by a steady-state at constant heat flux.

This analytical development of this single phase heat exchanges and its experimental validation on results from [21] are completely described in [6]. To put it in a nutshell, the total heat exchange coefficient is given by:

$$h(t,\tau) = \begin{cases} h_{conv} & \text{if } t < t_1 \\ \left(1 + \left(\frac{\lambda}{\sqrt{\alpha\tau}\,\mathrm{erf}\left(\sqrt{(t-t_1)/\tau}\right) h_{conv}}\right)^{2.4}\right)^{\frac{1}{2.4}} h_{conv} & \text{if } t \in [t_1; t_2] \\ \left(1 + \left(\frac{\lambda}{\left[2\sqrt{\alpha(t-t_2)/\pi} + \sqrt{\alpha\tau}\, e^{(t-t_2)/\tau}\left(1 - \mathrm{erf}\left(\sqrt{(t-t_2)/\tau}\right)\right)\right] h_{conv}}\right)^{2.4}\right)^{\frac{1}{2.4}} h_{conv} & \text{if } t > t_2 \end{cases} \quad (1)$$

Where t_1 is the beginning of the wall heat flux excursion, t_2 is the end of the excursion. h_{conv} is the steady-state convective heat exchange coefficient, given by a Sieder-Tate correlation [6]. τ is the excursion period, that is dynamically computed during the calculation in CATHARE2 as well as t_1 and t_2 [6]. The previous work [6] has led to characterize the uncertainty of this model which is related to the value of the exponent 2.4 showing that this heat transfer model agrees well with the Su et al.'s experiments for $n = 2.4 \pm 0.6$ (3σ).

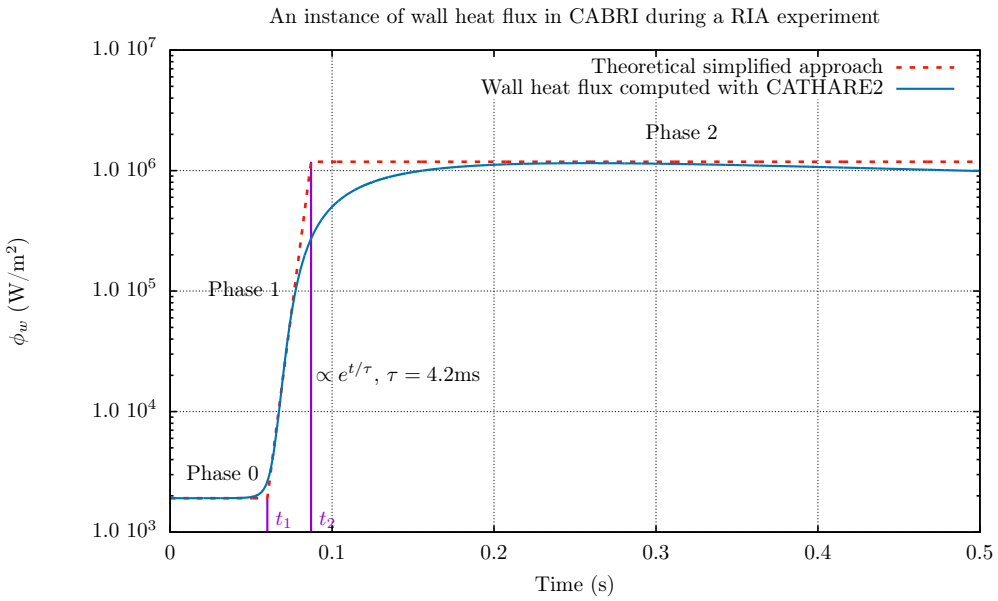

Figure 6: An illustration of the followed approach in the characterisation of heat exchanges during reactivity insertion transients

3.2 Correlation of Onset of Nucleate Boiling

As discussed in 2.2, the onset of nucleate boiling physics is complex and highly depends on the surface conditions. Furthermore, the onset of nucleate boiling point varies much as a function of the subcooling, of the Reynolds number and of the excursion period [21].

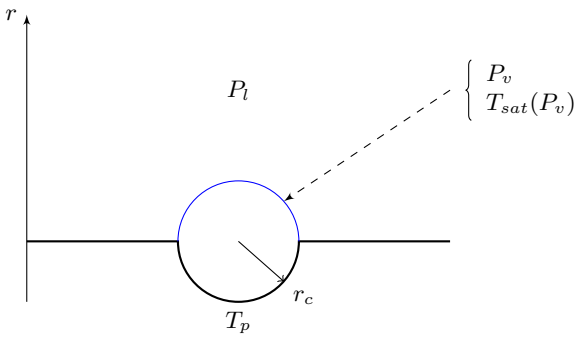

Figure 7: Bubble growing inside a nucleation site

In order to catch the physical behavior of these phenomena and to derive a model, the physical analysis of Sakuraï in [17] is considered (as already studied by Su et al. [21] in order to explain the trend of their experimental results). The Sakuraï's analysis takes into account the surface condition by considering the equilibrium criterion of a bubble in a nucleation site (cf. fig. 7) [24]. The temperature inside the bubble $T_l(r_c)$ is obtained assuming that the nucleation site is totally flooded. Taylor series at the first order lead to:

$$T_l(r_c) = T_w + r_c \left.\frac{\partial T}{\partial r}\right|_0 \tag{2}$$

The wall heat flux is yet written:

$$\phi_w = -\lambda_l \left.\frac{\partial T}{\partial r}\right|_0 = h\,(T_w - T_\infty) \tag{3}$$

and finally:

$$T_l(r_c) = T_w - \frac{hr_c}{\lambda_l}\left(T_w - T_\infty\right) \tag{4}$$

Sakuraï assumed that the bubble can appear and grow when the liquid temperature inside the cavity reaches T_{sat} at the pressure complying with the equilibrium criterion in equation 6.

$$T_{sat}(P_v) = T_{sat}\left(P_l + \frac{2\sigma}{r_c}\right) \tag{5}$$

$$P_v - P_l = \frac{2\sigma}{r_c} \tag{6}$$

with σ, the surface tension of water. Sakuraï obtained with the previous equations:

$$\Delta T_{sat} = T_w - T_{sat}(P_l) = \left(T_{sat}\left(P_l + \frac{2\sigma}{r_c}\right) - T_{sat}(P_l) + \frac{hr_c}{\lambda_l}\Delta T_{sub}\right)\frac{1}{1-\frac{hr_c}{\lambda_l}} \tag{7}$$

with $\Delta T_{sub} = T_{sat} - T_\infty$ representing the wall super-heat needed to reach the Onset of Nucleate Boiling. This analytical analysis allows to understand the variables that influence the phenomenon. Nevertheless, some parameters such as the nucleation site radius r_c are unknown.
Thus, based on that, for its implementation in CATHARE2, we have chosen to look for a model of ONB of the form:

$$\Delta T_{sat} = \left(a + \frac{h}{\lambda_l} b \Delta T_{sub}\right)\frac{1}{1-\frac{h}{\lambda_l}b} \tag{8}$$

where a and b are the parameters of the correlation which encompass the transient aspect and the subcooling. They have been determined from the experiments carried out by Su et al. [21] and summarized in table 1.

Table 1: Values of coefficients a and b derived from tests [21]

ΔT_{sub}	Re	a (K)	b (m)
10 K	60 000	4.54	11.84 10^{-6}
10 K	35 000	7.86	12.46 10^{-6}
25 K	60 000	1.83	10.39 10^{-6}
25 K	35 000	5.51	11.13 10^{-6}
25 K	25 000	5.66	11.77 10^{-6}
75 K	35 000	-10.17	8.88 10^{-6}
75 K	25 000	-4.06	8.10 10^{-6}

From table 1 we induce that b does not depend much on the Reynolds number. As a consequence, we derive:

$$b = -1.17\ 10^{-6}\Delta T_{sub}^{0.4} + 1.51\ 10^{-5} \tag{9}$$

Coefficient a depends on Re and ΔT_{sub}. After some steps, we propose:

$$a = k(Re)\Delta T_{sub}^{1.8} + w(Re) \tag{10}$$

Where coefficients k and w depend on Re :

$$\begin{cases} k(Re) = -2.91\ 10^{-5}\left(Re - 25000\right)^{1/2} - 4.78\ 10^{-3} & \text{(11a)} \\ w(Re) = -6.27\ 10^{-9}\left(Re - 37850\right)^2 + 8.26 & \text{(11b)} \end{cases}$$

To conclude, the Onset of Nucleate Boiling point in CATHARE2 is modified with the following correlation:

$$\Delta T_{sat_{ONB}} = \left[k(Re)\Delta T_{sub}^{1.8} + w(Re) + \frac{h(t,\tau)}{\lambda_l} b(\Delta T_{sub})\Delta T_{sub}\right]\frac{1}{1-\frac{h(t,\tau)}{\lambda_l}b(\Delta T_{sub})} \tag{12}$$

Where $h(t,\tau)$ is the single-phase heat exchange coefficient determined in the previous subsection. Results of this correlated model in comparison with the experiment are presented in fig. 8 with the associated data uncertainty. The experimental value is presented on x-axis, and the modeling one on y-axis. We can see that the correlation surrounds every experimental result at $\pm$ 25 %, including experimental uncertainties.

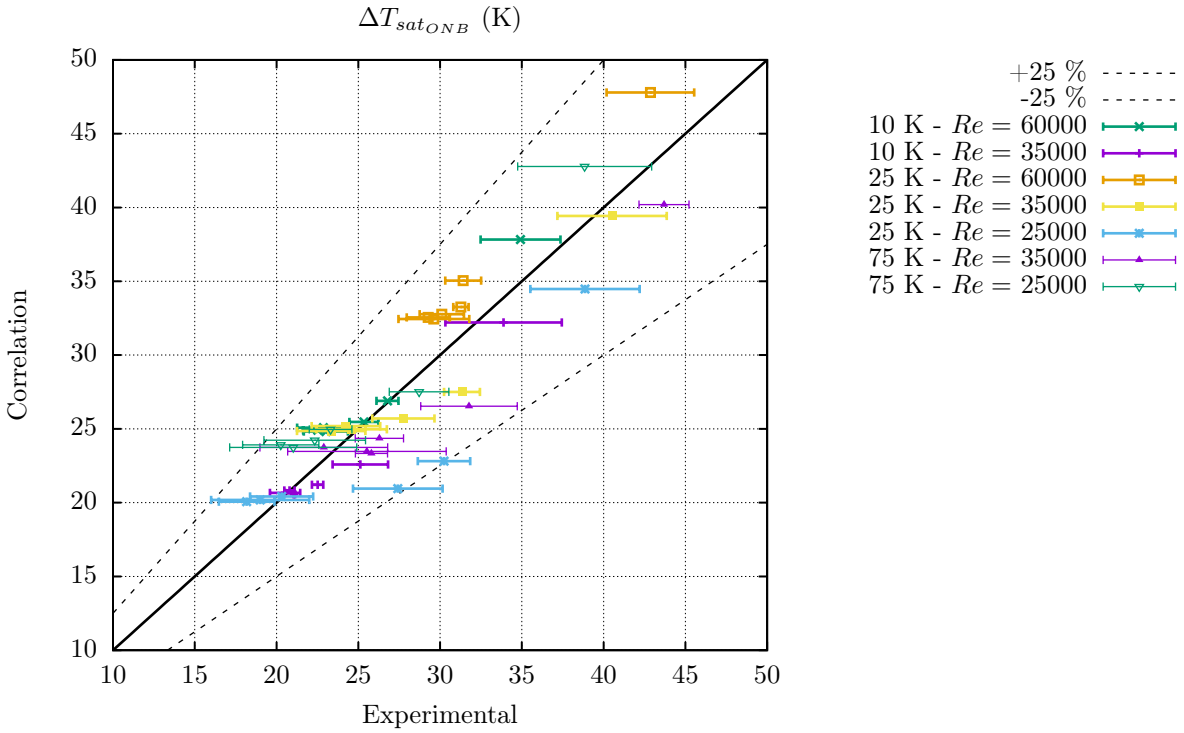

Figure 8: Results of the correlation (12)

Remark: This correlation does not depend on the pressure because the considered experimental tests have been made at atmospheric pressure. However, the ONB should depend on the pressure, given that coefficient a, corresponding to $T_{sat}\left(P_l + \frac{2\sigma}{r_c}\right) - T_{sat}(P_l)$ is not constant with pressure. Moreover, the phenomenon of bubble development in nucleation sites depends on the surface state and the material properties. We then found consistent values for b, corresponding to r_c, with orders of a ten of microns. This correlation is then not valid for high pressures and high wall rugosities.

3.3 Nucleate boiling heat exchanges for subcooled boiling

The heat exchanges in Fully-Developed Nucleate Boiling in transient conditions are also difficult to quantify, because the two-phase flow phenomenology in this regime is highly dependent on the wall temperature: small bubbles are formed at low temperatures and vapor columns are formed at high temperatures. It is then not possible to derive a unique analytical correlation valid for the whole domain of the nucleate boiling regime.

For sake of straightforwardness, a relation of type $\phi_{NB} = Cst\,(T_w - T_{ONB})^n$, with Cst is a constant and n a constant exponent, is sought for the implementation in CATHARE2 in case of transient conditions.

Fig. 9 presents the comparison between two experimental boiling curves issued from [20] and two theoretical curves obtained considering either the Thom modified correlation 13 or the Jens-Lottes modified correlation 14. In this figure, the plotted wall heat flux ϕ_w is given by the previous correlation for single phase heat exchanges ($h(t,\tau)$) before ONB and ϕ_{NB} in FDNB.

- the Thom correlation modified following the classical form $(T_w - T_{ONB})^2$ with k_{Thom} a constant:

$$\phi_{NB} = k_{Thom} \cdot h_{Thom}\,(T_w - T_{ONB})^2 = k_{Thom} \cdot h_{Thom}\,(T_w - T_{sat} - \Delta T_{sat_{ONB}})^2 \tag{13}$$

- The Jens-Lottes correlation modified :

$$\phi_{NB} = C\left(T_w - T_{ONB}\right)^4 = C\left(T_w - T_{sat} - \Delta T_{sat_{ONB}}\right)^4 \tag{14}$$

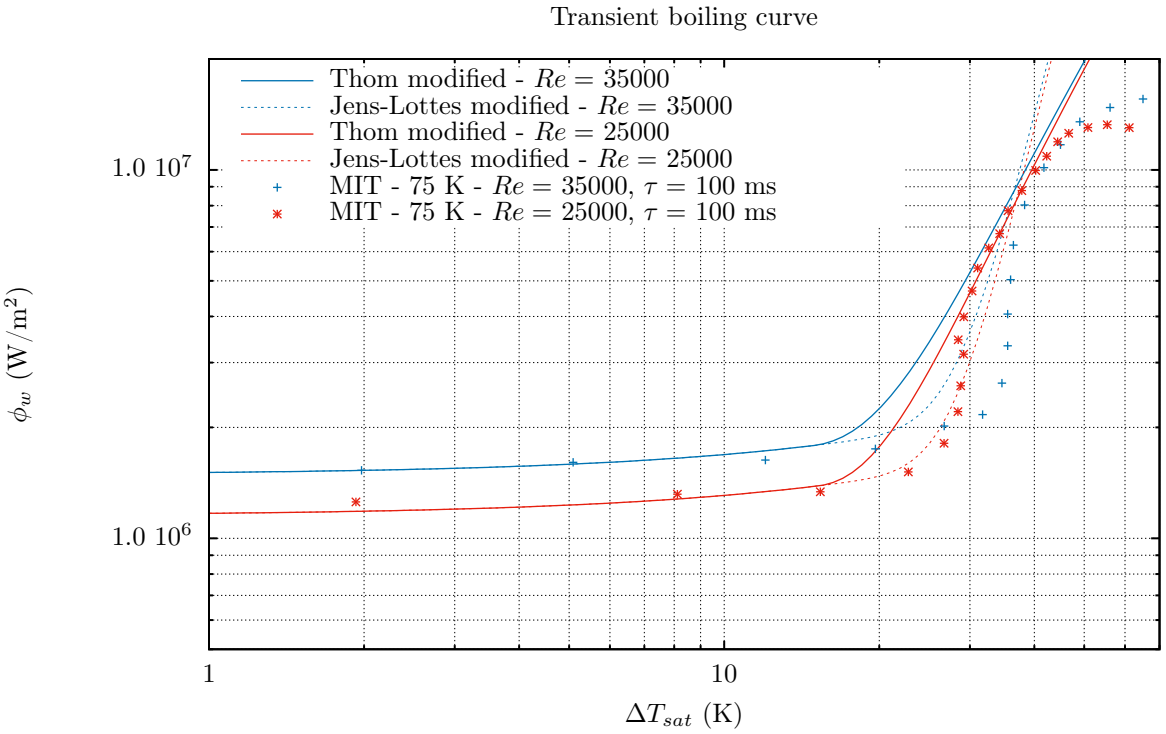

Figure 9: Comparison of two correlations to experimental curves for $\Delta T_{sub} = 75$ K and $\tau = 100$ ms from [22]

If the experimental results are of the type identified in the Thom's correlation $(T_w - T_{ONB})^2$ for high wall temperature, when vapor columns are already formed, the type of law identified in the Jens-Lottes modified correlation gives better adequacy on the whole FDNB regime. Moreover, [21] suggests a heat exchange law following ΔT_{sat}^4 with an adapted coefficient. And further studies of Kossolapov et al. [22] confirmed that trend. Based on these statements, the model of heat exchanges in Fully-Developed Nucleate Boiling implemented in CATHARE2 for transient conditions is based on a modified Jens-Lottes correlation where the coefficient C has been determined from results of [22] for different subcoolings. They are summarized in table 2.

Table 2: Value of coefficient C for the modeling of Fully-Developed Nucleate Boiling heat exchanges

ΔT_{sub}	C	Uncertainty
10 K	1.5	20 %
50 K	10.0	20 %
75 K	30.0	20 %

3.4 Critical heat flux

The used experimental study of the Departure from Nucleate Boiling in fast transients is presented in [22]. The critical heat flux is correlated on the basis of a non-linear superposition of effects, similar to the one used for single phase heat exchanges modeling :

$$\phi_{crit}(\tau, \Delta T_{sub}, P, G, X_{th}) = \left(\psi(\tau, \Delta T_{sub})^n + \phi_{crit_p}(P, G, X_{th})^n\right)^{\frac{1}{n}} \tag{15}$$

where the variable ψ contains the transient correction. This assumption is based on experimental observations of the evolution of the critical heat flux. When τ tends to 0, the critical heat flux does not depend on Re, but on the subcooling ΔT_{sub}. Moreover, the critical heat flux for $\tau \to 0$ tends to be proportional to $1/\sqrt{\tau}$ in [22]. And when $\tau \to +\infty$, the critical heat flux tends to its value in steady-state. ψ then gets the following form :

$$\psi(\tau, \Delta T_{sub}) = q(\Delta T_{sub}) \frac{1}{\sqrt{\tau}} \tag{16}$$

For small excursion periods, we deduce that:

$$q(\Delta T_{sub}) = -9.443 \frac{1}{\Delta T_{sub}} + 1.211 \tag{17}$$

n is then determined in equation (15) in order to get the physical evolution of ϕ_{crit} with τ:

$$\begin{cases} \phi_{crit}(\tau, \Delta T_{sub}, P, G, X_{th}) = \left(\psi(\tau, \Delta T_{sub})^4 + \phi_{crit_p}(P, G, X_{th})^4\right)^{\frac{1}{4}} & \text{(18a)} \\ \psi(\tau, \Delta T_{sub}) = \left(-9.443 \frac{1}{\Delta T_{sub}} + 1.211\right) \frac{1}{\sqrt{\tau}} & \text{(18b)} \end{cases}$$

Figure 10 gives the comparison between the experimental transient correction $\psi(\tau, \Delta T_{sub})$ and its model (eq. 18). This figure highlights that every test from MIT [22] is contained in the limit of ± 25 % around the value given by the model. To further assess the physical consistency of this correlation, additional experimental results have been drawn: NSRR tests and Sakuraï tests [18]. We can see that these results, that was not used for the development of the model, are well reproduced by this model too. So we conclude that:

- the transient correction $\psi(\tau, \Delta T_{sub})$ does not depend on the geometry. In fact, MIT experiment are made with a plane wall, NSRR tests are performed with rods and Sakuraï experiments with a platinum wire heater;
- this correlation seems to be valid for low pressures, until 10 bar. Indeed, Sakuraï tests that are presented are performed at 5 and 7 bar.

Remark: As for the Onset of Nucleate Boiling, there are some reasons to think that the Critical Heat Flux (and more particularly the transient correction) depends on the pressure. This assessment is based on the Serizawa model [29] and Pasamehmetoglu [30] work, that determines analytically the energy needed to vaporize the liquid layer between the wall and the vapor layer resulting of the merge of the vapor columns in transient conditions. This energy embraces, among other, the latent heat of vaporisation that depends on the pressure. This correlation is then invalid for pressure higher than 10 bar, and for liquid subcooling lower than 10 K.

4 SPERT-IV reactor and CATHARE2 modeling

4.1 SPERT-IV reactor

As already explained in the introduction, the SPERT-IV reactor, whose power is mostly mitigated by moderator effect and not Doppler effect, enables the occurrence of boiling regimes up to the Critical Heat Flux. The results of SPERT-IV reactor are thus considered for the validation of the two-phase heat transfer models in transient conditions. To achieve this validation on Separated Effect Tests, where only thermal-hydraulics influences the clad temperature, neutronics feedbacks are not simulated, imposing the experimental power in the simulations.

SPERT (Special Power Excursion Reactor Test) is a program, initiated in 1954, designed to study the effects of RIA on the kinetics of the core, on the fuel integrity and on the thermal-hydraulics. It provides many experimental data for both thermal-hydraulics and neutronics during fast power excursions. SPERT-IV experiment aimed at studying the response of the core to a reactivity insertion. The particularity of this

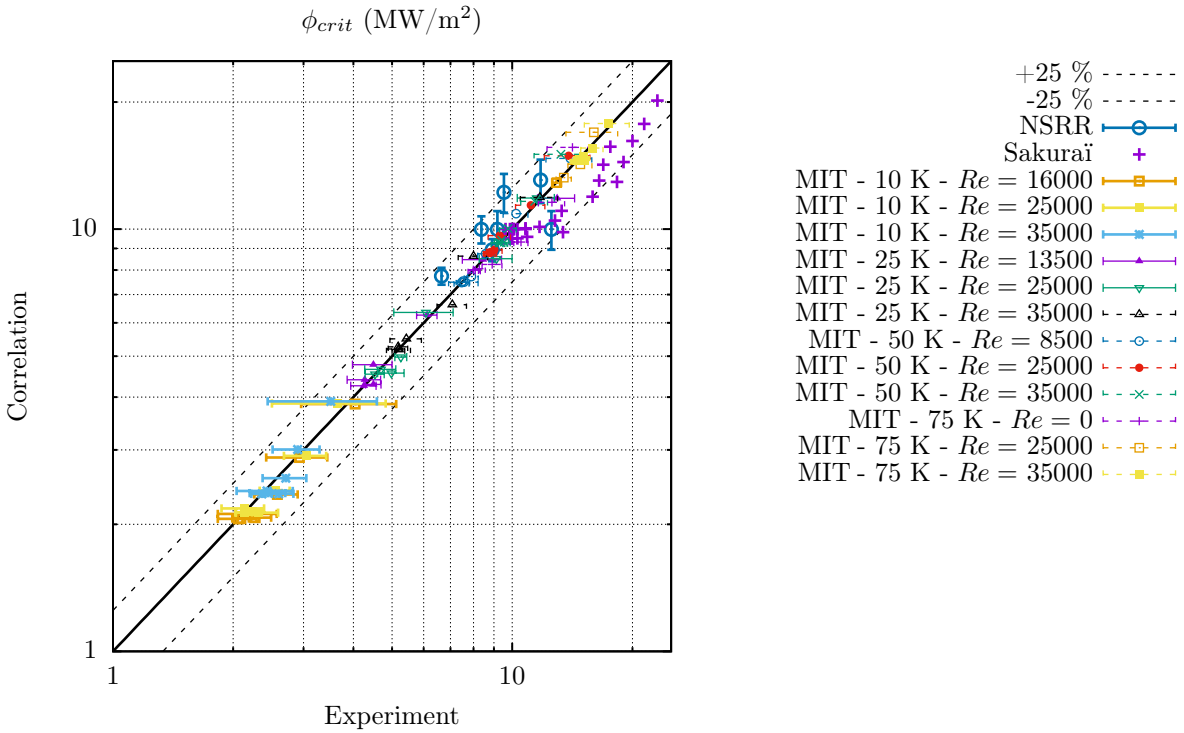

Figure 10: Results of correlation (18)

facility is that it allows a parametric investigation of the core response in regard of a variation of the power excursion period, the water flow rate and the pressure.

SPERT-IV reactor is a light water-cooled and moderated pool type reactor with provisions for both upward forced and natural convection cooling. The core is composed of 25 standard fuel assemblies in a square five by five section. The core and assemblies configurations are provided in fig. 11.

Each standard fuel assembly contained 12 removable fuel plates, with highly enriched U-Al alloy ($\approx$ 93 % of ^{235}U). Assemblies consist in fuel plates surrounded by a can. Four gang operated boron-alloy double-blade control rods and one transient rod of the same style located in the center of the core are accommodated in the standard fuel assembly replacing its six fuel plates. In order to initiate the transient, the transient rod is dropped. The complete specification of the reactor components is described in [12]. There are 39 transient tests reported for SPERT-IV reactor benchmark analysis [12]. The published results for peak power, peak cladding temperature, and energy released are provided in the document [12] with respect to a number of control variables such as initial reactor power, reactivity insertion, bulk moderator-coolant temperature, hydrostatic head, and coolant circulation rate. The tests performed in SPERT-IV reactor at 1 bar are then made with manageable conditions:

- inlet mass flowrate (0-315.5 l/s);
- initial power (0.001-1 W);
- external reactivity (0.80-2.14 $).

Five groups of tests have been performed imposing different flow rates (table 3). And, each test among these groups differ with respect to initial ambient reactor temperature, power, reactivity insertion, and corresponding transient period. It is also apparent that the tests in each group were performed in a progressive manner by increasing the amount of positive insertion of reactivity so the corresponding transient period is shorter. Most of the tests were initiated with critical reactor at a power level of approximately 1 W and an initial transient period superior to 15 ms. The remaining tests were performed with periods inferior to

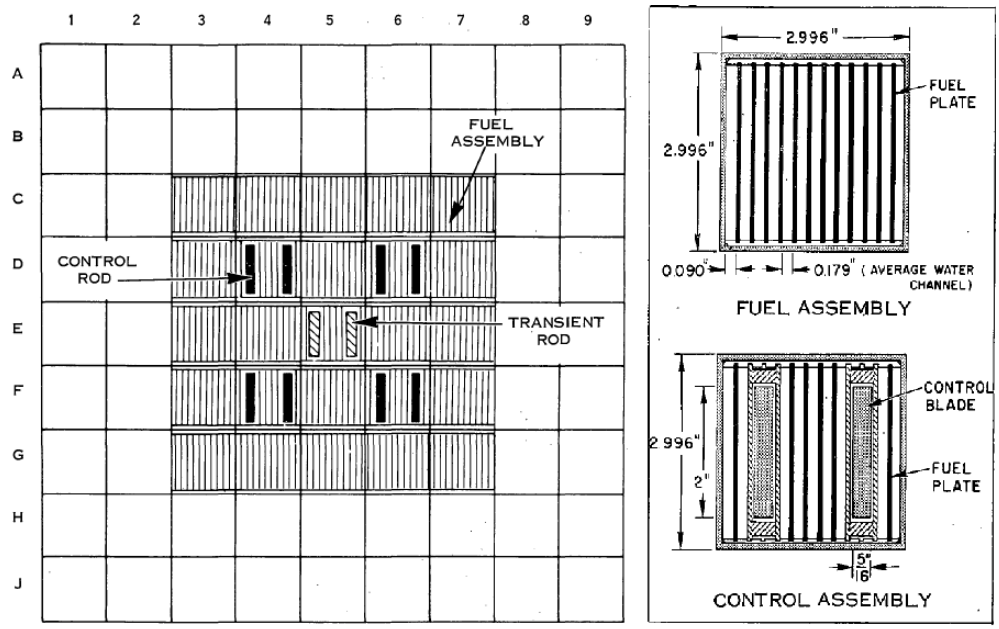

Figure 11: Left : View of SPERT-IV core - Right : standard and controlled fuel assemblies [12]

Table 3: Groups experimental flow rates

Group	flow rate [l/s]	coolant velocity [m/s]
1	0	0
2	31.5	0.365
3	63.1	0.731
4	157.7	1.828
5	315.5	3.657

15 ms for which the reactor is initially subcritical at a power in the milliwatt range. This initial condition allows the complete reactivity insertion before power rises to a significant level.

Given that the fuel is highly enriched, Doppler feedback effect is really negligible in comparison with other feedbacks effects, due to clad expansion and moderator thermal expansion (feedback coefficient (20–35°C): -1.2 ¢ of reactivity per °C) and void (-41.5 ¢ per % decrease in moderator density) [13]. Some measurements are available too and are very interesting for a validation purpose.

In the present framework of validation of boiling thermal hydraulic models devoted to fast transients, SPERT-IV tests with, as well natural circulation as forced upward coolant flows, are taken into account. The considered validation matrix considered for CATHARE2 is composed of the tests with the highest reactivity insertion in each group of tests 4.

Table 4: Simulated tests among SPERT-IV D-12/25 [31]

Test	Group	Maximal power (MW)	Energy deposit (MJ)	External reactivity ($)	Flow rate (l/s)	power excursion period (ms)
B16	1	875	8.5	2.14	0	7.0
B23	2	435	5.97	1.80	31.5	10.1
B29	3	425	6.05	1.80	63.1	10.4
B33	4	435	6.13	1.80	157.7	10.0
B39	5	505	6.08	1.80	315.5	10.1

For every test, the clad temperature measurement, compared to the simulation results in the next section,

is performed on assembly E5, containing the transient rods (cf. fig. 11), at 3 or 4 inches below the core center line.

4.2 CATHARE2 code

The CATHARE2 code was previously adapted to the simulation of fast insertion reactivity transients where Doppler effect plays a predominant role and validated on several CABRI tests [5–7]. New developed models presented in section 3 have been implemented in CATHARE2 code. The excursion period τ is evaluated, in an explicit way, throughout the simulation as it was done in [5] with ϕ_w is the wall heat flux:

$$\frac{1}{\tau} = \frac{1}{\phi_w}\frac{\mathrm{d}\phi_w}{\mathrm{d}t} \tag{19}$$

This period is calculated over the first ten time steps of the excursion in order to stabilise the calculation. From previous work [5], it comes that, during the exponential excursion, the total heat exchange tends very fast to a limit value, only depending on τ. As a consequence, the logarithmic derivative of the flux does not depend on the convective heat exchange in the eq. (19) and τ is computed as:

$$\frac{1}{\tau} = \frac{1}{T_w - T_\infty}\frac{\mathrm{d}(T_w - T_\infty)}{\mathrm{d}t} \tag{20}$$

To validate the implemented transient two-phase heat exchange in CATHARE2 on SPERT-IV reactor benchmark calculations, the SPERT-IV core is modelled in a multi-1D representation considering one channel per assembly. Considering the symmetries inside the core, this leads, realistically, to model only 6 flow channels as presented in table 5. The heated length being of 0.61m, 61 axial meshes are considered.

Table 5: Core modelling characteristics

Channel	Assembly (cf. fig. 11)	Weight	Fuel plate number
1	E5	1	6
2	F5	4	12
3	F6	4	6
4	G5	4	12
5	G6	8	12
6	G7	4	12

The geometry of each assembly (with specific flow area, heating and friction perimeter) is taken into account. An additional channel represents the pool without the core, connected to the lower box and the upper box, and allows the natural convection to set up. The mass flow rate is implemented as a boundary condition on the lower box. The upper box is connected to an atmospheric pressure boundary condition. The heated length of the assemblies is set to the experimental one (2 ft i.e. 0.61m). The global core power, which is imposed in these CATHARE2 simulations, is provided by IAEA and the axial and radial power profiles have been drawn from literature [13, 32] and from measurements [31, 33].

5 Simulation results of SPERT-IV

In order to assess the models of two-phase heat exchanges in fast conditions presented in section 3, five simulations of SPERT-IV transients with CATHARE2 have been carried out with imposed power (table 4). These tests have been chosen because they are the fastest transients available in SPERT-IV experiments, with an external reactivity around 2 \$. Experiments with lower reactivity insertions and thus higher power excursion periods do not experience two-phase flow as it is demonstrated on transients B34 and B35 in section 5.1.
The five selected tests (table 4), with high reactivity insertion, would thus allow to obtain a very fast increase of wall heat flux and then a quite low heat flux excursion period. As a consequence, two- phase flow develops and the effect of the transient heat exchanges models presented in this paper should be maximal. The heat

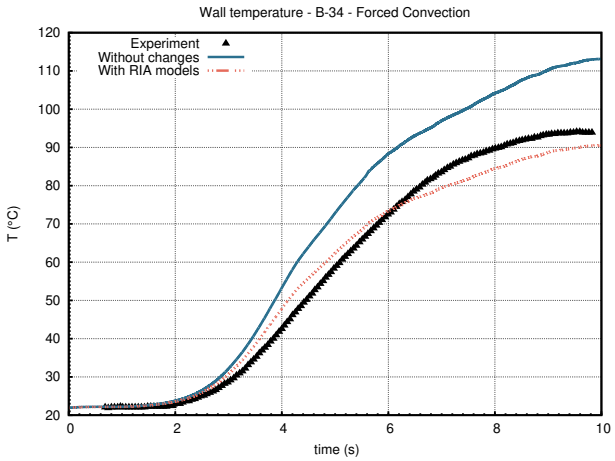

Figure 12: B34

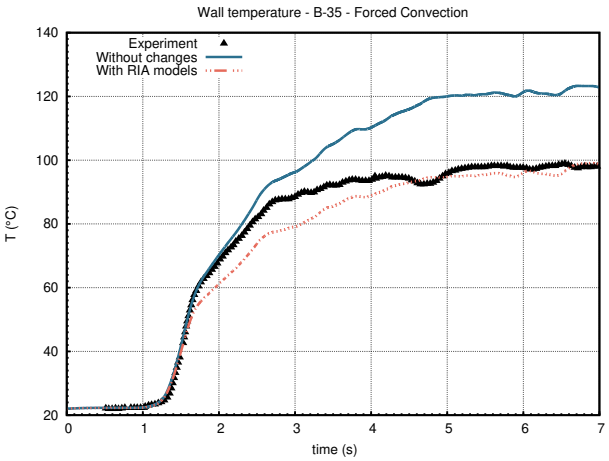

Figure 13: B35

flux excursion period (τ eq. 19,20), involved in the models proposed in this paper, should be different from the experimental power excursion period owing to the effects of fuel heat conduction and core thermal inertia.

For each of these SPERT-IV tests, a Best Estimate simulation is first performed with models given in section 3 (sec. 5.1). Uncertainty propagation studies are also achieved and discussed in section 5.2.

5.1 Best-estimated results

The Best Estimate simulation of each test is carried out with the extended version of CATHARE2 with models given in section 3 (sec. 5.1) and is compared to experimental results as well as results obtained keeping initial standard models.

First of all, two results of tests B34 and B35 in forced convection (with the highest flow rate) and low reactivity insertion are presented in figures 12 and 13. The experimental conditions of these tests are reported in table 6.

Table 6: Single-phase tests

Test	Maximum power (MW)	External reactivity ($)	Flow rate (l/s)	power excursion period (ms)
B34	-	0.88	315.5	516
B35	9.8	1.05	315.5	104

In these two tests, no boiling appears and transient heat transfer only occurs in single-phase flow. The heat flux excursion periods (τ eq. 20) simulated are 539 ms and 106 ms in test B34 and B35, respectively. They are consistent with the experimental power excursion periods of 516 ms and 104 ms, respectively. That is coherent with the low inertia and high conductivity of the SPERT-IV fuel plates. Indeed, under these considerations, the power is proportional to the temperature rise such as $\rho C_p \frac{dT}{dt} \sim P(t)$ with $P(t) \sim P_0 e^{t/\tau}$ and the heat flux excursion, i.e. wall temperature excursion (-eq. (19) rewritten in eq. (20)-) could be approximated by $T(t) \sim P_0 \frac{\tau}{\rho C_p} e^{t/\tau}$, with the same period.

The transient single-phase heat transfer 1, already assessed on CABRI tests [6], gives simulation results in very good agreement with experimental data of test B34 and B35 much closer than the results obtained with the standard CATHARE2 code. In figures 12 and 13, experimental and simulation results are compared. Among the simulation results, the results 'without changes' refer to the standard CATHARE2 code and 'RIA' to the version with new models described in section 3. It is worthwhile mentioning that the wall temperature evolution is better simulated. As the heat flux excursion period increases the transient heat

flux reaches steady-state value given by a Sieder-Tate's correlation [6]. This correlation is a modified form of the Dittus-Boelter's correlation (which is in the standard CATHARE2 code [1]) adapted to high gradient temperature between the wall and the fluid bulk (characteristic of fast reactivity insertion transients). In this case, it is necessary to account for the variation of the fluid viscosity with temperature. Hence, RIA'models give better results even in quasi-static conditions, i.e. power excursions presenting large periods.

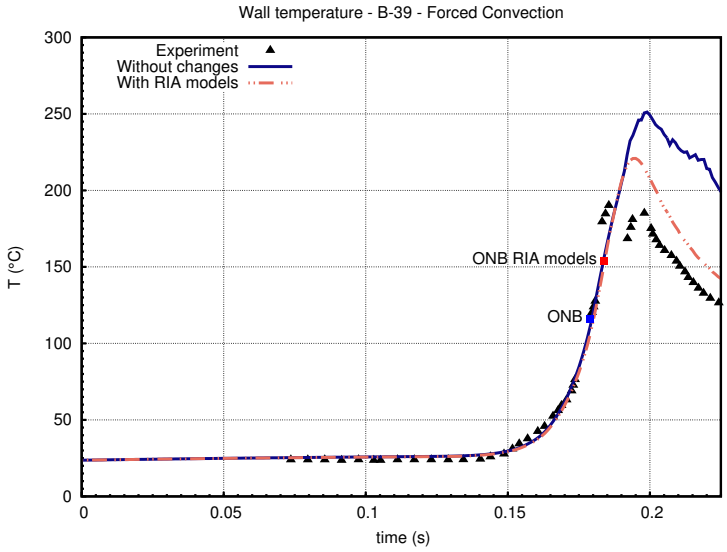

Figure 14: B39 - Wall temperature

Focusing on the five tests with high reactivity insertion and boiling occurrence (table 4), the test B39 at the higher flow rate, and the test B16 in natural circulation, are presented through a detailed analyses. Indeed, the other three tests (B23, B29 and B33) display the same physical behavior than test B39 in forced convection. The comparison of these simulation results with the experimental results are given in next section 5.2.

The evolution of the clad temperature in the test B39 under forced convection (315.4 l/s) is displayed in figure 14. The simulated wall temperatures obtained with and without the new models of section 3, show that the models elaborated for transient conditions improve the consistency between the experimental and simulation results. The wall temperature peak is better simulated as well as its evolution. The Onset of Nucleate Boiling in both cases are also plotted in this figure. This onset is postponed with the new models; it is delayed in comparison with standard calculation. It comes also from figure 16 that the void fraction at the location of interest (on assembly E5 at 3 or 4 inches below the core center line) is lower with the new models ($\sim -20\%$ than with the standard version where void fraction peaks reach $\sim 40\%$). In figure 15, wall heat fluxes in single-phase and two-phase regimes as well as the critical heat flux, obtained from equation 18, are plotted. It is observed that the critical heat flux is reached in the simulation with the standard CATHARE2 and not reached with the new RIA models. It is consistent with the literature assessment (section 1). The single-phase and the boiling heat fluxes are larger with the new models (a factor 2 in single-phase flow and ~ 1.3 for boiling regime where the void fraction in twice lower than without these models). The simulated heat flux excursion period (τ) is 8.5 ms which is close to the experimental power excursion periods of 10.1 ms.

Clad temperature evolution is also very well simulated with the new models in test B16 in natural convection, without flow rate (figure 17). This result is in better agreement. The Critical Heat Flux is not reached; i.e. before 0.145s. The heat flux increase, due to the nucleate boiling heat exchanges, is then significantly delayed in comparison with standard calculation. The Onset of Nucleate Boiling (ONB) occurs latter when considering the new models. In spite of this, the peak of temperature is well reproduced. From the examination of void fraction and wall heat fluxes at the same location (figures 19 and 18), it comes that a high void fraction (of nearly 100%) and the critical heat flux are reached in both simulations even though the critical heat flux with new models is twice higher than using the standard correlations. This result highlights

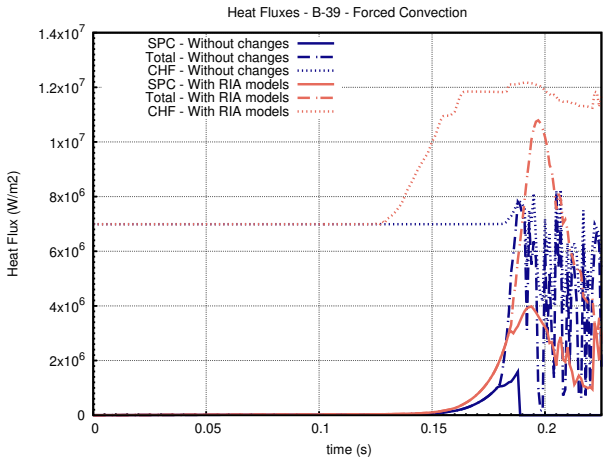

Figure 15: B39 - Wall heat fluxes -SPC: Single Phase Convection, Total: single-phase + two-phase regimes

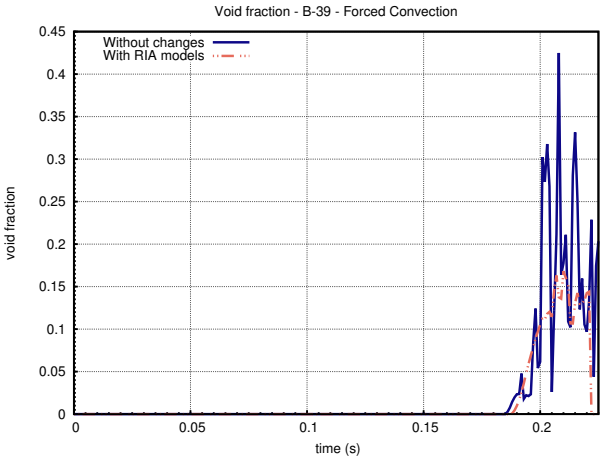

Figure 16: B39 - Wall void fraction

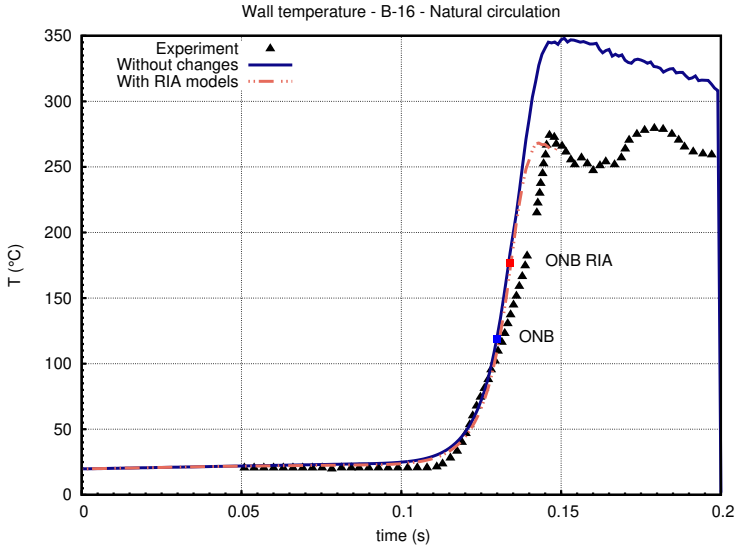

Figure 17: B16 - Wall temperature

a favorable field for the critical heat occurrence in natural circulation. After the heat critical flux occurrence with new models, the results are no more meaningful owing that no new model for transient heat flux in the transition regime (after critical heat flux) has been developed. So the simulation with RIA models stops.

Finally, the simulated heat flux excursion period (τ) is 4.12 ms which is close to the experimental power excursion periods of 7.0 ms.

5.2 Uncertainty propagation

In order to study the influence of the uncertainties associated to the new RIA models, which have been determined in the previous section on the main results, an uncertainty propagation study has been achieved. It is based on 100 simulations performed according to a Latin Hypercube Sample and Gaussian distribution uncertainty laws (from expert judgment) on the four developed models in section 3.

- The uncertainty on the single phase heat exchange coefficient concerns the coefficient 2.4 of equation (1). Its Gaussian distribution has a mean of 2.4 and a standard deviation (σ) of 0.2, leading a value of 0.6 for

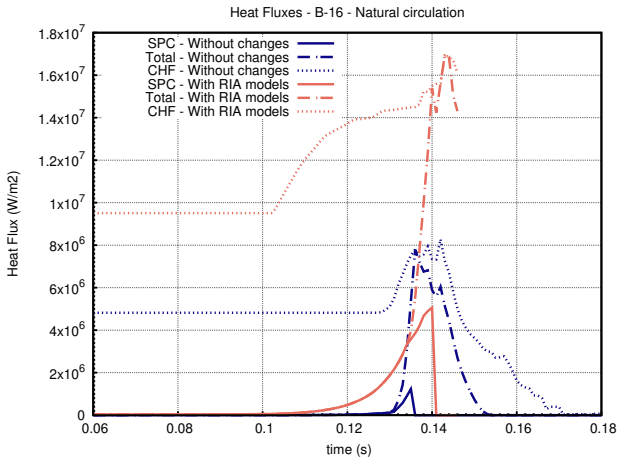

Figure 18: B16 - Wall heat fluxes -SPC: Single Phase Convection. Total: single-phase + two-phase regimes

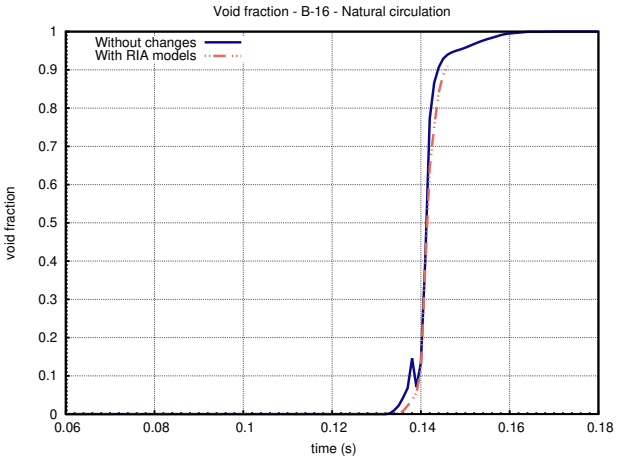

Figure 19: B16 - Wall void fraction

3σ ;

- the uncertainty on the ONB occurrence is put on $\Delta T_{sat_{ONB}}$ (eq. 12), which a mean value given by this model and a standard deviation of 0.09, leading a value of around 25% for 3σ ;
- the uncertainty on the heat transfer in Fully-Developed Nucleate Boiling is put in ϕ_{NB}. It is characterized by a mean value given by this model (equation (14) and a standard deviation σ of 0.07, leading a value of around 20% for 3σ;
- Finally, the uncertainty on the Critical Heat Flux is a Gaussian law of mean value given by equation (18) and a standard deviation of 0.09, leading a value of around 25% for 3σ;

For each of these SPERT-IV tests (table 4), the comparison of experimental and simulation results obtained with new RIA models and standard version for the clad temperature evolution on assembly E5 is displayed.

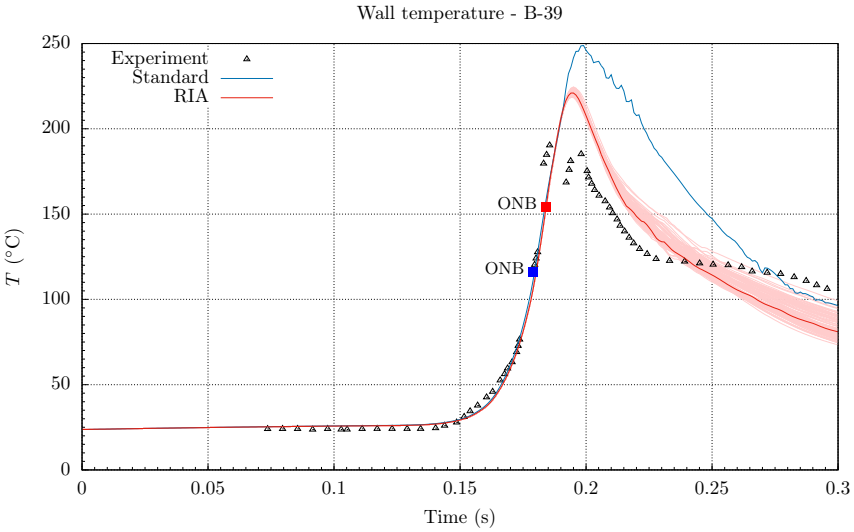

Figure 20: B39 - Wall temperature. Comparison of experimental and simulation results -standard: without new models - RIA: with new models of section 3.

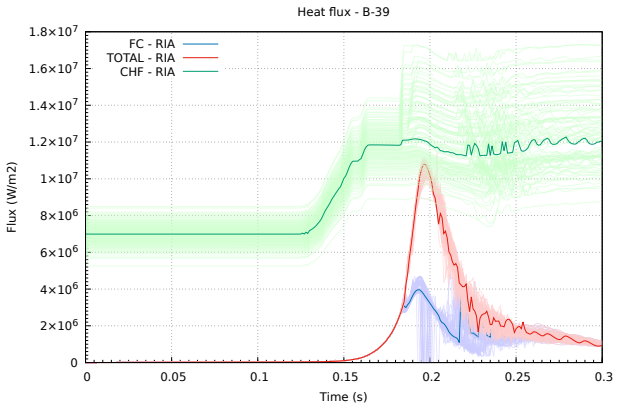

Figure 21: B39 - Heat fluxes -FC: single phase Heat flux, -TOTAL: single and two-phases regimes -CHF: Critical Heat Flux

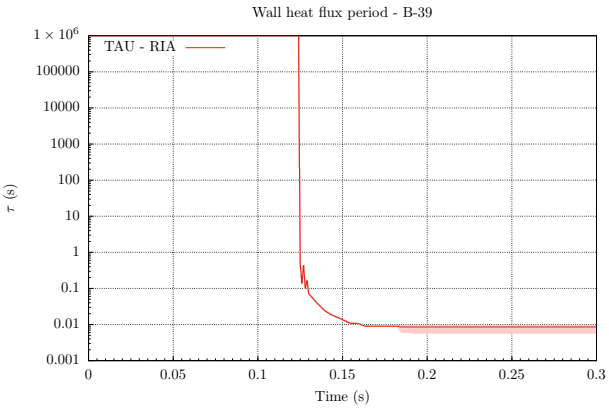

Figure 22: B39 - Heat flux excursion period

For test B39, wall temperature simulation results obtained with the new models of section 3 and the standard version are plotted in figure 20. The 100 BEPU simulations results are drawn in red (a deep red line for the Best Estimate result, already presented in section 5.1, and lighter red lines for the other uncertainty propagation results). From this figure, it appears that for any result obtained taking into account the uncertainties on the new models adapted to RIA transient, the wall temperature peak as well as the temperature decrease after this peak are in better agreement with the experimental result than the result obtained with the standard version of the code. The models uncertainties lead to a small variation of the wall temperature decrease after the peak. This is related to the evolution of the wall heat fluxes (figure 21) which presents more variations linked to the models uncertainties after the ONB. In this figure, wall heat fluxes in single-phase and two-phase regimes as well as the critical heat flux are plotted for the 100 simulations performed with the new RIA models (deep line is Best Estimate result and lighter lines correspond to other uncertainty propagation results). It appears that the heat exchanges are first in single-phase flow up to 0.18s and then in two-phase regime before reverting back to single-phase heat exchanges after around 0.24s. A part of the variability of the wall heat flux in the various regimes is also linked to the variability of the heat flux excursion period computed through equation (20). An illustration of the evolution of τ over the course of this transient B39 is given in figure 22. A high initial value of τ, in no way influencing the transient, is arbitrary fixed at the beginning. As soon as the clad temperature evolves (fig. 20), the τ drops and reaches a stable value at around 0.15s at the beginning of the power excursion. At around 0,18s, the τ only slightly varies with the considered uncertainties. Due to the large variability of the critical heat flux, a part ($< 10\%$) of the BEPU simulations reaches the critical heat flux. Finally, it can be underlined that the variations of the wall total heat flux, due to the proposed models uncertainties, do not have a large influence on the wall temperature.

Wall temperature results obtained for the other selected SPERT-IV tests are reported in figures 23, 24, 25 and 26 for the wall temperature evolution at various flow rates.

In figures 23, 24 the differences between results obtained with standard and new model are small but the new models give however results closer to the experimental results. The models uncertainties only lead to small discrepancies. This difference is larger on the peak temperature in test B23, where the peak obtained with the new model is about 25 °C lower than with the standard models. Nevertheless in these three tests, the experimental peak seems to be postponed to larger times and the temperature doesn't decrease after. This behaviour should be further investigated in regards to the comprehension of the physical behaviour during these tests and the measurements uncertainties. One must note that the digitization of data from [12] cannot provide a great accuracy. It has also been checked that the simulated heat flux excursion periods (τ) are in the order of magnitude of the experimental power excursion periods; 3.9ms, 3.26ms, 2.49ms in Best Estimated simulations compared to 10ms, 10.4ms and 10.1 for tests B33, B20 and B23, respectively.

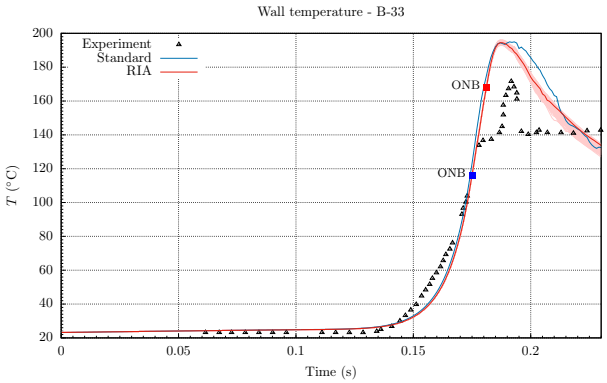

Figure 23: B33 - Wall temperature

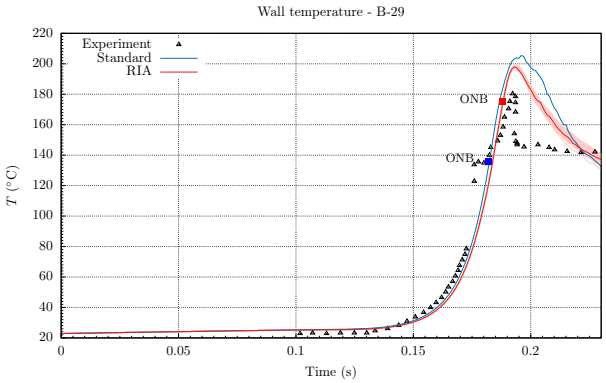

Figure 24: B29 - Wall temperature

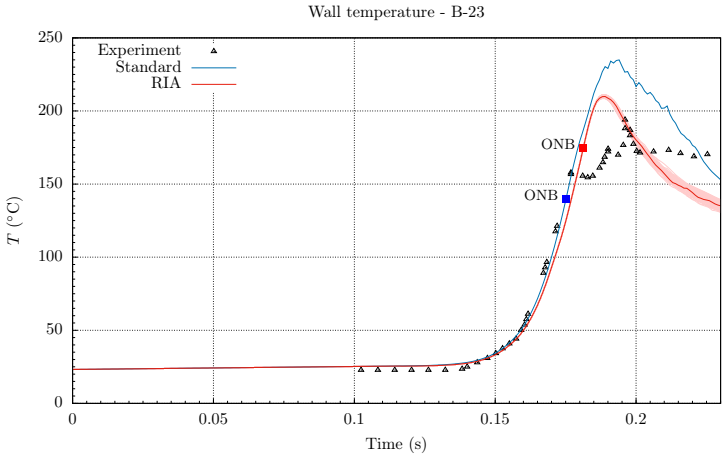

Figure 25: B23 - Wall temperature

In the B16 test, performed in natural convection without flow rate, the Critical heat flux is reached in most of the uncertainty propagation simulations (figure 27). Results of Best Estimate Plus Uncertainty study for the wall temperature in this test are presented in figure 26. With the standard models, the wall temperature is overestimated of about 80°C. The critical heat flux is reached, what leads to the transition boiling and to under saturated film boiling regimes. The wall is covered by a vapor film that insulates the clad. The calculated void fraction reaches a value of 0.9 (figure 19. That explains why the temperature decreases so slowly after the peak. In results obtained considering new models, the maximal temperature is quite lower than with standard models and are very close to the experimental one. It results from that a total heat flux between clad and water much higher with new models. Once again, even if the considered models uncertainties induce wall heat flux variations, they do not have a large influence of the wall temperature which remains around the experimental value. Finally, given that the boiling curve in CATHARE2 has not been modified after the CHF, the calculation is stopped after the CHF.

6 Conclusion and prospects

Pursuing an ultimate aim of having predictive multi-physics tools for the simulation of Reactivity Initiated Accidents in reactor, a great deal of effort have been made to improve the models of the CATHARE2 code and validate it on Separate Effect Test and Integral experiments.

The challenge is thus to succeed the simulation with this CATHARE2 tool of these various multi-physics

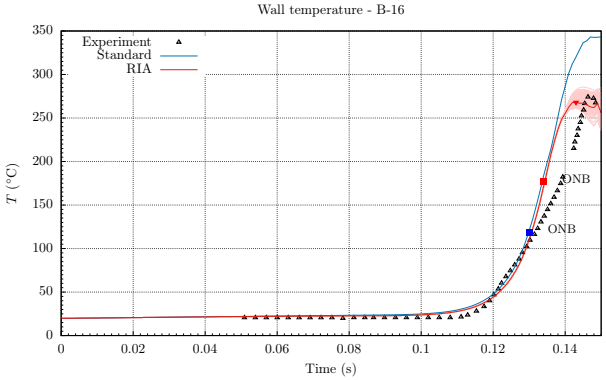

Figure 26: B16 - Wall temperature

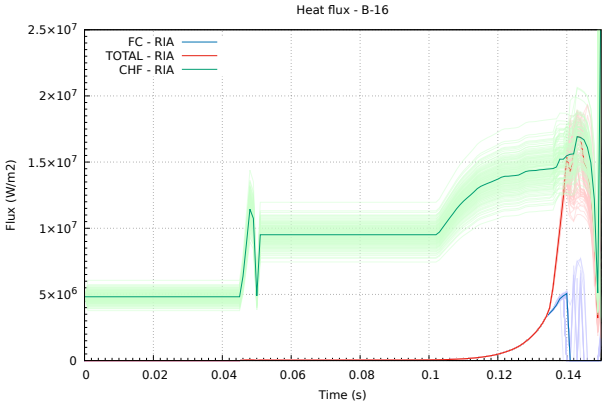

Figure 27: B16 -Heat fluxes -FC: single phase Heat flux, -TOTAL: single and two-phases regimes -CHF: Critical Heat Flux

transients catching the governing multi-physic phenomena . Indeed, these transients embrace fast phenomena under thermal-hydraulics, thermal-mechanics and neutronics coupling. After having reviewed the current capabilities of the CATHARE2 tool in regard to the main influential phenomena occurring during such RIA transients (established from a QPIRT), main improvements have been achieved [5] [6] and [7]. This extended version of CATHARE2 has been validated on various reactivity insertion tests realized in the CABRI reactor involving fast transients under single-phase liquid flow regimes [5]. The next step for the simulation of complex fast RIA in reactors was the modeling and validation of the heat transfers in transient boiling regimes which have a huge impact on the wall heat fluxes. From a literature review, a boiling curve, up to the Critical Heat Flux, has been derived from past RIA separate effects tests. It is characterized by four variables; a single phase heat exchange coefficient in single phase regime, the wall temperature for the ONB occurrence, the heat flux in Fully-Developed Nucleate Boiling and the Critical Heat Flux. Ranges of model uncertainty were associated to these variables. These new models adapted to fast transient have been implemented in CATHARE2 and validated on SPERT-IV experiments with different flow rates (one experiment was in natural convection without flow rate). Indeed, SPERT-IV fuel presenting a low $^{238}U/^{235}U$ ratio, the transient power is governed by neutronic moderator feedback and allows boiling inception during these tests. By imposing the power evolution, these tests enable the sole validation of the wall heat transfers with the wall temperature as output variable of interest. Five two-phase flow SPERT-IV tests have been simulated considering the propagation of the model uncertainties on the introduced four variables. Calculated transient wall temperatures have been compared to experimental results. Results considering the new models are in better agreement than with the standard models and very close to the experimental ones. The uncertainty propagation does not lead to large uncertainties on wall temperature. The B16 test in natural convection reaches the Critical Heat Flux (considering standard or news models) and its results obtained with the new models agree with experimental results up to this point.

Given that the thermal-hydraulics during RIA is better simulated with the new set of correlations, it could be interesting to study the core kinetics of SPERT-IV reactor. Indeed, the feedback effects will be slightly different in amplitude and time, and will influence the power calculation of the core. As an example, the moderator temperature is higher before the peak with new correlations than it is with standard correlations, and lower after the peak. This changes the shape of the moderating feedback evolution.

Finally conclusions are drawn on the validation state of this extended CATHARE2 version for fast RIA transients The results that represent the state of modeling allow concluding that introduced models in CATHARE2 are able to simulate such RIA tests of SPERT-IV involving fast transient boiling. Furthermore, validating a code is a continuous process that is worth pursuing in order to improve the models with an aim of obtaining the best simulation results. To explain and reduce the difference between calculated and experimental values, further efforts then must be paid. Models for transition boiling and film boiling regime should be elaborated to complete the boiling curve in fast RI transient to simulate the end of test experiencing

Critical Heat Flux. Moreover, simulations of SPERT-IV tests with, this time, a coupled neutronic feedback would be performed to validate this extended version of CATHARE2 on these integral multi-physic tests. For some tests, the pressure measurement outside the core is available, helping to detect the massive production of void fraction inside the core. It could also be interesting in a next validation step to interpret, if it is possible, the pressure measurements performed outside of the core to figure out an order of magnitude of the core void fraction and compare it to our simulation results.

References

[1] G. Geffraye, O. Antoni, M. Farvacque, D. Kadri, G. Lavialle, B. Rameau, and A. Ruby. CATHARE 2 V2.5_2: A single version for various applications. *Nuclear Engineering and Design*, 241(11):4456–4463, November 2011.

[2] IAEA. IAEA CRP 1496 (2008-2013) innovative methods in research reactors analysis: Benchmark against experimental data and neutronics and thermal-hydraulics computational methods and tools for operation and safety analysis of research reactors, Technical Report: Technical reports series no. 480.

[3] IAEA. Research reactor benchmarking database: Facility specification and experimental data. Technical Report Tech. Rep. Technical Reports Series No. 480, International Atomic Energy Agency, 2015.

[4] S. Chatzidakis, A. Ikonomopoulos, and S. E. Day. PARET-ANL Modeling of a SPERT-IV Experiment Under Different Departure from Nucleate Boiling Correlations. *Nuclear Technology*, 177(1):119–131, January 2012.

[5] J.-M. Labit, N. Marie, E. Merle, and O. Clamens. Multiphysics CATHARE2 modeling and experimental validation methodology against CABRI transients. *Nuclear Engineering and Design*, 373, 110836, https://doi.org/10.1016/j.nucengdes.2020.110836, 2021.

[6] J-M. Labit, N. Marie, E. Merle, and O. Clamens. Transient heat exchanges under fast reactivity insertion accident. *Nuclear Engineering and Design*, 373, 110917, https://doi.org/10.1016/j.nucengdes.2020.110917:1–13, 2021.

[7] J.-M. Labit, N. Seiler, E. Merle, and O. Clamens. Nusselt correlation development in unsteady laminar gas flows for CABRI multiphysic simulations with CATHARE2. *Nuclear Engineering and Design*, 373, 111032, https://doi.org/10.1016/j.nucengdes.2020.111032, 2021.

[8] RELAP5/MOD3.2 code manual. Technical Report Report NUREG/CR-5535, US Nuclear Regulatory Commission, Washington DC, USA, 1995.

[9] H. Austregesilo and others. ATHLET models and methods. Technical Report Report GRS-P-1/Vol. 4, Gesellshaft fur Anlagen und Reaktorsicherheit, Garching, Germany, 2003.

[10] J. Staudenmeier. TRACE: TRACE/RELAP advanced computational engine 2004. In *Transactions of the 2004 nuclear safety research conference*, number NUREG/CP-0188, pages 25–27, oct 2004.

[11] V. Bessiron, T. Sugiyama, and T. Fuketa. Clad-to-Coolant Heat Transfer in NSRR Experiments. *Journal of Nuclear Science and Technology*, 44(5):723–732, May 2007.

[12] S. Day. SPERT IV D-12/25: Facility specification. February 2015.

[13] N. H. Badrun, M. H. Altaf, M. A. Motalab, M. S. Mahmood, and M. J. H. Khan. Modeling of SPERT IV Reactivity Initiated Transient Tests in EUREKA-2/RR Code. *International Journal of Nuclear Energy*, 2014/167426, December 2014.

[14] M. Kaminaga. EUREKA-2/RR: A computer code for the reactivity accident analyses in research reactors. *JapanAtomicEnergy Agency.*

[15] W. L. Woodruff, N. A. Hanan, and J. E. Matos. A comparison of the RELAP5/MOD3 and PARET/ANL codes with the experimental transient data from the SPERT IV D-12/25 series. In *Proceedings of the International Meeting on the Reduced Enrichment for Research and Test Reactors*, USA, June 1997.

[16] Margulis M. and E. Gilad. Simulations of SPERT-IV D12/15 transient experiments using the system code THERMO-T. *Progress in Nuclear Energy.*

[17] A. Sakurai and M. Shiotsu. Transient Pool Boiling Heat Transfer—Part 1: Incipient Boiling Superheat. *Journal of Heat Transfer*, 99(4):547–553, November 1977.

[18] A. Sakurai and M. Shiotsu. Transient Pool Boiling Heat Transfer—Part 2: Boiling Heat Transfer and Burnout. *Journal of Heat Transfer*, 99(4):554–560, November 1977.

[19] M. W. Rosenthal. An Experimental Study of Transient Boiling. *Nuclear Science and Engineering*, May 1957.

[20] G-Y. Su, M. Bucci, T. McKrell, and J. Buongiorno. Transient boiling of water under exponentially escalating heat inputs. Part I: Pool boiling. *International Journal of Heat and Mass Transfer*, 96:667–684, May 2016.

[21] G-Y. Su, M. Bucci, T. McKrell, and J. Buongiorno. Transient boiling of water under exponentially escalating heat inputs. Part II: Flow boiling. *International Journal of Heat and Mass Transfer*, 96:685–698, May 2016.

[22] A. Kossolapov. *Transient flow boiling and CHF under exponentially escalating heat inputs*. PhD thesis, Massachusetts Institute of Technology, 2018.

[23] A. Kossolapov, F. Chavagnat, R. Nop, N. Dorville, B. Phillips, J. Buongiorno, and M. Bucci. The boiling crisis of water under exponentially escalating heat inputs in subcooled flow boiling at atmospheric pressure. *International Journal of Heat and Mass Transfer*, 160(120137), 2020.

[24] Y. Y. Hsu. On the size range of active nucleation cavities on a heating surface. *Journal of Heat Transfer*, 14:67–82, 1971.

[25] W. H. Jens and P. A. Lottes. Analysis of heat transfer, burnout, pressure drop and density date for high-pressure water. Technical report, Argonne National Lab., 1951.

[26] T. Fujishiro, K. Yanagisawa, K. Ishijima, and K. Shiba. Transient fuel behavior of preirradiated PWR fuels under reactivity initiated accident conditions. *Journal of Nuclear Materials*, 188:162–167, June 1992.

[27] A. Sakurai, M. Shiotsu, K. Hata, and K. Fukuda. Photographic study on transitions from non-boiling and nucleate boiling regime to film boiling due to increasing heat inputs in liquid nitrogen and water. *Nuclear Engineering and Design*, 200(1):39–54, August 2000.

[28] R. Nop. *Experimental investigation and modeling of the transient flow boiling crisis of water at moderate pressure and high subcooling*. PhD thesis, Universite Paris-Saclay, 2020.

[29] A. Serizawa. Theoretical prediction of maximum heat flux in power transients. *International Journal of Heat and Mass Transfer*, 1983.

[30] K. O. Pasamehmetoglu, R. A. Nelson, and F. S. Gunnerson. Critical heat flux modeling in forced convection boiling during power transients. *Journal of Heat Transfer*, 112:1058–1062, 1990.

[31] J. G. Crocker, J. E. Koch, Z. R. Martinson, A. M. McGlinsky, and L. A. Stephan. Nuclear start-up of the SPERT IV reactor.

[32] A. Hainoun, N. Ghazi, F. Alhabit, S. Bourdon, et al. *SPERT-IV Benchmark Problem Consolidation Report for the IAEA CRP 1496*, page 177. 12 2019.

[33] J. G. Crocker and L. A. Stephan. Reactor power excursion tests in the SPERT-IV facility.